 SDHM, vol.9, no.3, pp.217-232, 2013

Crack Tip Parameters Under Large Scale Yielding Condition

F. Caputo[1], G. Lamanna[1] and A. Soprano[1]

Abstract: In recent years, the study of the behaviour of damaged structures has been focusing on cracked components in presence of an extensive material yielding at the crack tip; under this condition, linear elastic fracture mechanics theory is not able to describe the real stress-strain state at the crack tip and consequently either the static or the fatigue behaviour of the component. In this work, an extensive parametric numerical analysis of the plastic zone size and shape at the crack tip for a through cracked plate under Mode I loading condition is presented. The obtained results allow assessing the limits of the linear elastic fracture mechanics in presence of an extensive material yielding at the crack tip and the relationships between the plastic zone size and other parameters of the elastic plastic fracture mechanics theory are pointed out.

Keywords: EPFM, Large Scale Yielding, plastic radius.

1 Introduction

The behaviour of damaged structures is usually studied through the Linear Elastic Fracture Mechanics (LEFM), which considers only plane stress-strain states at the crack front.

The main advantage of two-dimensional theories is their analytical simplicity compared to the three-dimensional ones, but for Large Scale Yielding (LSY) phenomena they aren't able to overcome some limits in describing the actual behaviour of the material around the damage.

In fact, one of the basic principles of the LEFM theory is to consider the Plastic Zone Size (PZS) at the crack tip as negligible with respect to the crack length, i.e. to take into account Small Scale Yielding (SSY) condition [Park, Kim, Lee and Rheem (1996)]. To overcome this limit and to consider the stress-strain state transition from plane stress to plane strain condition several studies introduce a

[1] The Second University of Naples, DIII, Italy.

stress constraint factor, experimentally, numerically [Cisilino, Aliabadi, and Otegui (1998); Cisilino and Aliabadi (1999)] or analytically derived, which influences the yielding stress value [Chang and Hou (2005)].

Other studies emphasized the thickness influence on the stress-strain state at crack tip: in Kudari, Maiti, and Ray (2009) the evaluation of PZS through both microhardness technique and Finite Element Method (FEM) shows how the PZS, determined in the plane of the through crack (i.e. plastic radius, r_p) on the outer surface of a plate specimen, increases as the thickness decreases.

In any case, LEFM theory can't describe the behaviour of "short cracks" [McDowell (1997)] and it can't even lead to accurate predictions when applied to most 3D geometries [Bellett, Taylor, Marco, Mazzeo, Guillois and Pircher (2005)].

In the first case, the conditions for LEFM parameters application are not met because the state of stress at the short crack tip is generally characterized by a Large Scale Yielding (LSY) and high ratios of PZS to the crack length [Hussain (1997)] are found.

Several numerical and experimental investigations [Zhang and Du (2001), Caputo, Lamanna, and Soprano (2006, 2011-2, 2012-3, 2013-2)] have shown that such ratio is larger for short cracks than for long ones, for a given nominal Stress Intensity Factor (SIF) and that if PZS is considered as the governing parameter of crack growth behaviour higher rates are to be expected for short cracks than for long ones, which is consistent with the experimental observations.

Moreover, in the case of short cracks further effects related to the material microstructure can also take place and influence the stress-strain state at the crack tip and the growth rate [Jin and Mall (2003)]. In Lados, and Apelian (2008) it has been shown that the changes in crack growth mechanisms can also be explained by correlating PZS with the material microstructural features.

For these reasons, in the recent years, a particular attention is being paid to the behaviour of damaged structures [Benedetti and Aliabadi (2013); Sfantos and Aliabadi (2007)] either in presence of high values of remote loads [Armentani, Citarella, and Sepe (2011); Citarella, Cricrì and Armentani (2012); Caputo, Di Gennaro, Lamanna, Lefons and Riccio (2013)] or in presence of short cracks, when a relatively large scale yielding condition occurs around the crack tip.

The difficulties encountered to describe the stress-strain state at the crack tip through the parameter of LEFM theory is leading to consider the Elastic-Plastic Fracture Mechanics (EPFM) theory's parameters [Leitao, Aliabadi, and Rooke (1995)], as the CTOD (Crack Tip Opening Displacement), the CTOA (Crack Tip Opening Angle), the COD (Crack Opening Displacement) and the J-integral [Newman, James and Zerbst (2003); Rice, and Rosengren (1968)].

In Werner (2012), CTOD and COD are used to evaluate PZS and to describe the crack growth rate in presence of high load values.

PZS strictly depends on many variables, such as the material yield stress (σ_s), the applied remote load (described by the J-integral parameter for elastic-plastic conditions), the crack size (a) and the component thickness (t), but an analytical formulation for PZS such as to take into account all these parameters is not yet available, exactly because of the difficulties in computing the stress-strain field which exists ahead of the tip of a growing crack.

In particular, those difficulties arise as the size and the shape of the plastic zone depend on the adopted yield criterion and on the thickness of the considered component [Camas, Garcia-Manrique and Gonzalez-Herrera (2011); Amiri, Belhouari, Bounoua, Achour and Bouiadjra (2013); Narasimhan and Rosakis (1998)], which in turn influence the stresses at the crack tip.

The main scope of the study reported in the present paper is to describe the elastic-plastic state of stress and strain, which takes place around the crack tip under Mode I loading condition, by using the parameters of EPFM theory (among which the PZS is considered), as well as it is possible to describe the elastic stress-strain state through LEFM theory's parameters.

The analysis of the behaviour of a crack under Mode I loading condition can be related to the fact that, as also showed in Gao, Wang, Kang, and Jiang (2010), the Mode I loading condition has a crucial effect on the plastic zone size and shape also in mixed mode loading conditions.

2 Analytical background

According to the LEFM theory and considering a through transversal crack in an infinite plate subjected to a remote longitudinal stress (Mode I) the PZS can be represented by the following equations, respectively in plane stress and in plane stress condition:

$$\begin{aligned} PZS(\theta) &= \frac{1}{4\pi}\left(\frac{K_I}{\sigma_s}\right)^2\left(1+\frac{3}{2}\sin^2\theta+\cos\theta\right) \\ PZS(\theta) &= \frac{1}{4\pi}\left(\frac{K_I}{\sigma_s}\right)^2\left(\left(1-2\nu^2\right)(1+\cos\theta)+\frac{3}{2}\sin^2\theta\right) \end{aligned} \tag{1}$$

where K_I is Mode I stress intensity factor, θ is the polar coordinate ,σ_s is the material yield stress and ν is the Poisson module. For $\theta = 0$ and $\nu = 0.3$, equations (1)

become:

$$\begin{cases} r_{p\_LEt} = \dfrac{K_I^2}{2\pi\sigma_s^2} & \text{plainstrain} \\ r_{p\_LEd} = \dfrac{K_I^2}{2\pi(2.5\sigma_s)^2} & \text{plainstrain} \end{cases} \tag{2}$$

According to Irwin and Dugdale approaches [Anderson (1995)], PZS in the plane of a through crack is respectively given by:

$$r_{p\_Ir} = \frac{K^2}{\pi\sigma_s^2} \qquad r_{p\_Dug} = \frac{\pi}{8}\left(\frac{K_I}{\sigma_s}\right)^2 \tag{3}$$

In 1968 Rice presented the J-integral parameter [Rice and Rosengren (1968)], a path-independent contour integral for the analysis of the stress state at crack tip and he showed that the value of this integral is equal to the energy release rate parameter for a nonlinear elastic cracked solid.

Considering an arbitrary counter-clockwise path (Γ) around the crack tip, the J-integral is given by:

$$J = \int_\Gamma \left(W dy - T_i \frac{\partial u_i}{\partial x} ds\right) \tag{4}$$

where W is the strain energy density, y is the normal to the crack direction x, T_i are components of the traction vector, u_i are the displacement vector components and ds is a length increment along contour Γ. Considering a power law relationship between plastic strain and stress, Hutchinson (1968) and Rice, and Rosengren (1968) showed that the J-integral parameter characterizes crack tip stress state in a nonlinear elastic material.

For the special case of a linear elastic material and Mode I loading condition the J-integral is given by:

$$J = \frac{K_I^2}{E'} \qquad \text{with} \qquad E' = \begin{cases} E & \text{planestrain} \\ \dfrac{E}{1-\nu^2} & \text{planestrain} \end{cases} \tag{5}$$

According to Broberg (1999) the J-integral parameter regards only a plane stress or a plane strain condition and then in presence of a finite thickness plate the J-integral parameter value can be calculated either in the middle plane of the plate, where the stress-strain state is very close to a plane strain one, or on the outer surfaces.

3 Description of the numerical model

The examined component is a plate with a trough crack in the middle transverse section subjected to a remote longitudinal stress (Mode I), whose value spans the range $1 \div 352$ N/mm^2 (Fig. 1); the allowed ranges of the geometrical and physical parameters considered for the component are those illustrated in Tab. 1.

Table 1: Investigation parameters

parameters	W	L	a	t	σ
	[mm]	[mm]	[mm]	[mm]	[MPa]
	50	100	$0.1 \div 10$	$0.5 \div 5$	$0 \div 352$

The material properties used in the model have been assumed to be non linear (Fig. 2). Elastic-plastic analyses of FE model have been performed by using Abaqus® ver. 6.11 FE code.

The FE models (Fig. 3) have been built with a number of nodes between 64826 and 180855 and a number of elements between 14520 and 42090, depending on the values assumed by the geometrical parameters.

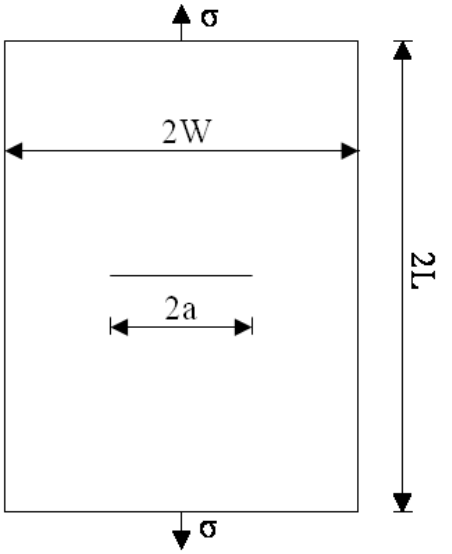

Figure 1: Test case geometry.

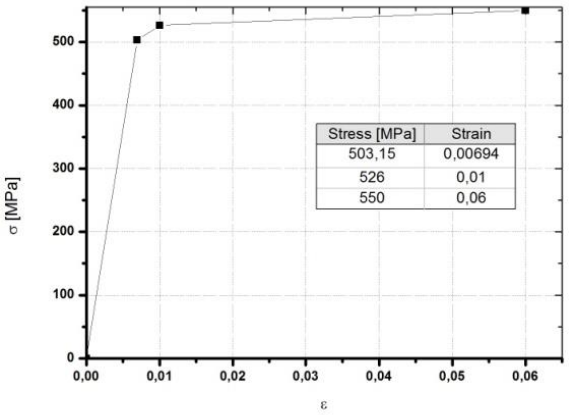

Figure 2: Material properties.

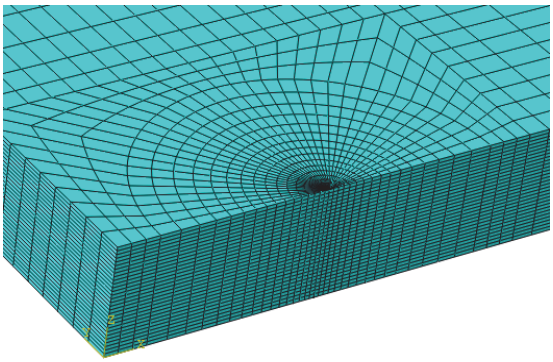

Figure 3: FE model detail at crack tip.

Symmetry conditions have been used for an efficient computation and therefore a quarter symmetric model has been adopted. The reduced integration 20-nodes brick elements (element type C3D20R by the Abaqus® elements' library) have been used. In all models, the element sizes have been kept accurately small to match with those necessary at the crack tip (where the minimum average element length is about 1E-04mm) to reach the required resolution of the stress field. Twenty elements have been considered along the thickness to resolve consistently the out of plane stress gradient.

In this paper, the plastic radius (r_p), i.e. the plastic zone size on the crack plane, in the middle plane of the plate, has been evaluated through the von Mises yield

criterion, by considering the distance from the crack front at which the von Mises stress, σ_{vm}, reaches the value of the material yielding stress, σ_s = 503.15 MPa (Fig. 4).

The numerical J-integral parameter has been evaluated in the middle plane of the plate by using the Virtual Crack Extension (VCE) technique [Caputo, Lamanna, Lanzillo, and Soprano (2013)], as implemented in the algorithms of the Abaqus® code.

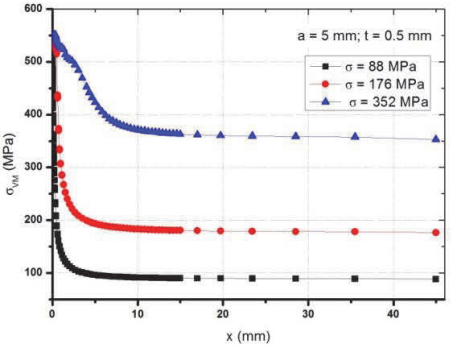

Figure 4: σ_{vm} vs distance from crack front (x) @ a = 5 mm, t = 0.5 mm

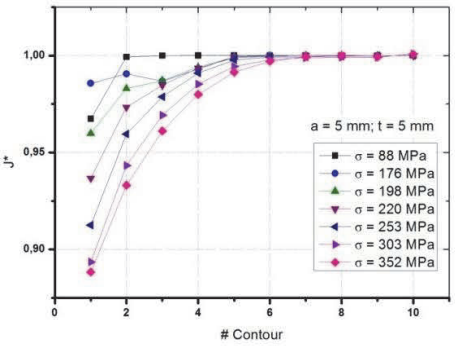

Figure 5: J/J_{10} vs # Contour @ a = 5 mm, t = 5 mm

Provided that the crack faces are parallel to each other, the J-integral parameter value should be independent of the domain used, but J-integral parameter values estimated at different ring paths (contours) can vary because of the approximate nature of the finite element solution; the actually considered J-integral parameter value is that one appearing approximately constant from one contour to the next one (Fig. 5).

4 Analysis of results and conclusions

Figs. 6 and 7 show the influence of both geometrical and boundary parameters (plate thickness, t, remote stress, σ, crack length, a) on the J-integral parameter values, J. It can be seen that, as well as expected, the increase of both σ and a, for a fixed t, leads to an increase of J, while for a fixed σ, the increase of t leads to a decrease of J. Figs. 8 and 9 show that for a fixed a, the increase of σ leads to an increase of J, while the increase of t implies a decrease of J.

Comparing the evolution of the J-integral parameter value calculated by finite element method through the Abaqus® code, J_Aba, with either that one evaluated analytically through the LEFM theory, J_LE, or that one evaluated analytically by

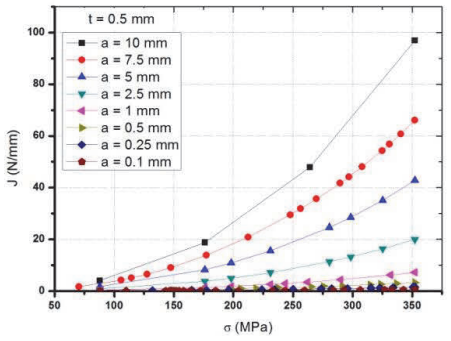

Figure 6: J vs σ @ t = 0.5 mm

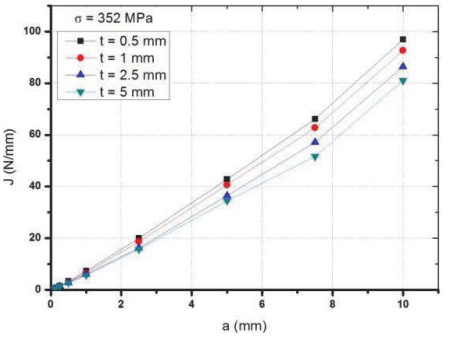

Figure 7: J vs a @ σ = 352 MPa

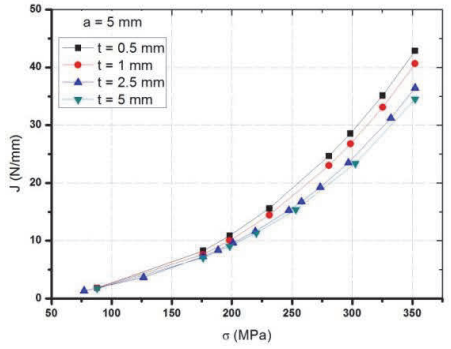

Figure 8: J vs σ @ a = 5 mm

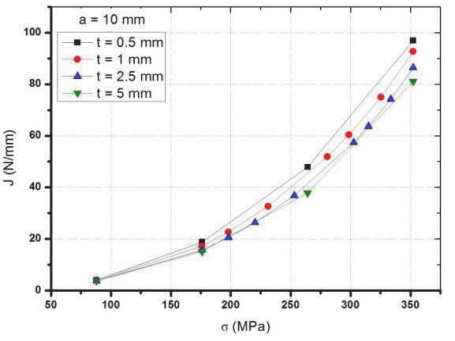

Figure 9: J vs σ @ a =10 mm

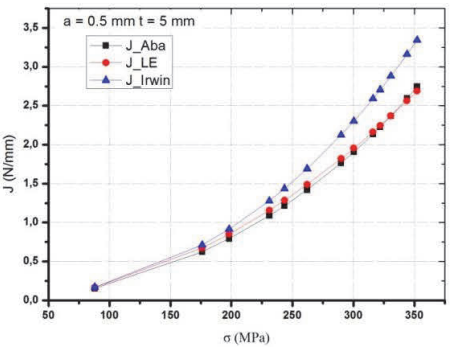

Figure 10: Comparison of J vs σ @ a = 0.5 mm, t = 5 mm

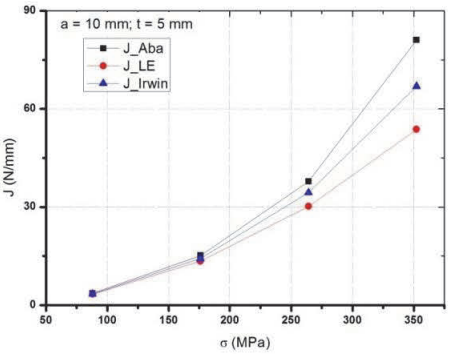

Figure 11: Comparison of J vs σ @ a = 10 mm, t = 5 mm

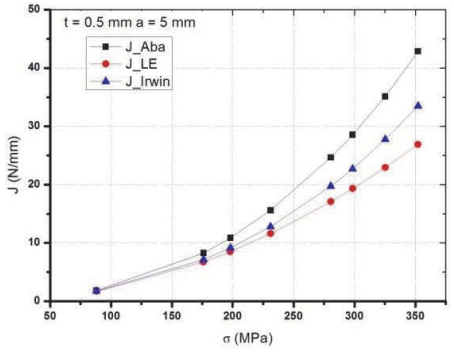

Figure 12: Comparison of J vs σ @ a = 5 mm, t = 0.5 mm

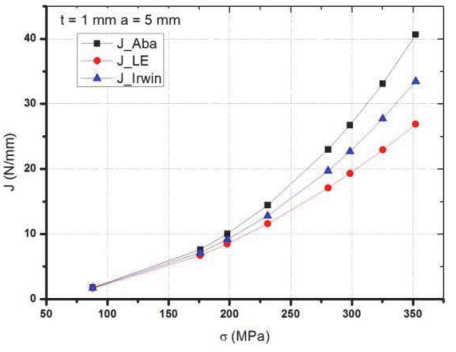

Figure 13: Comparison of J vs σ @ a = 5 mm, t = 1 mm

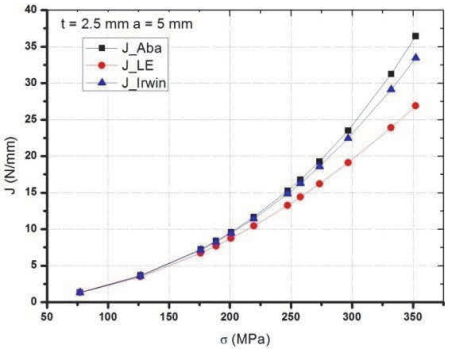

Figure 14: Comparison of J vs σ @ a = 5 mm, t = 2.5 mm

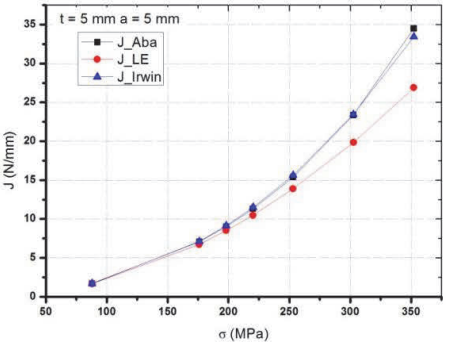

Figure 15: Comparison of J vs σ @ a = 5 mm, t = 5 mm

considering the Irwin correction factor, J_Irwin, it can be seen from the plot of Fig. 10 that the J_LE values are well in agreement with the J_Aba values in presence of SSY (i.e. short cracks with high value of t).

The J_Irwin values in the same conditions are higher than both of them.

Moreover, considering long cracks with high remote load values (i.e. LSY condition), J_Aba values are higher than J_LE values, even if the Irwin correction factor is considered (Fig. 11).

In Figs. from 12 to 15 it can be seen that, for a fixed a, the difference between the J_Aba values and the J_LE values decreases when the thickness increases, i.e. by approaching to SSY conditions.

As already mentioned and as it is shown in the following figures, this behaviour can be explained by the extension of PZS: if PZS is negligible with respect to the crack

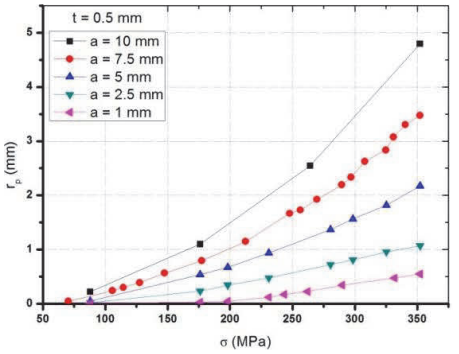

Figure 16: r_p vs σ @ t = 0.5 mm (long crack)

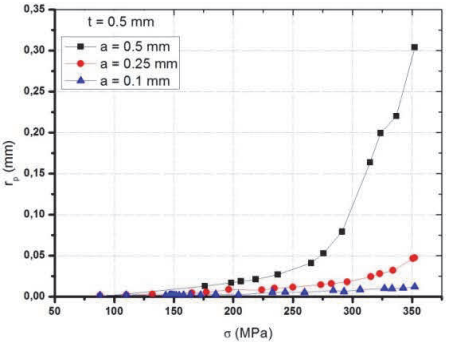

Figure 17: r_p vs σ @ t = 0.5 mm (short crack)

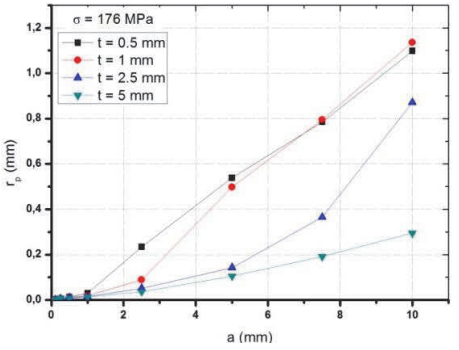

Figure 18: r_p vs a @ σ = 176 MPa

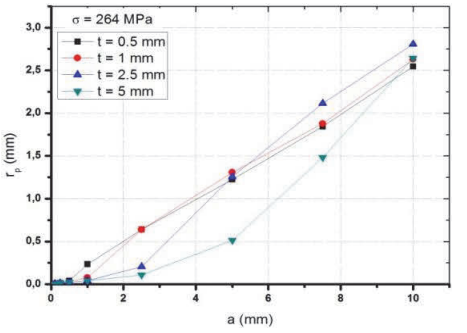

Figure 19: r_p vs a @ σ = 264 MPa

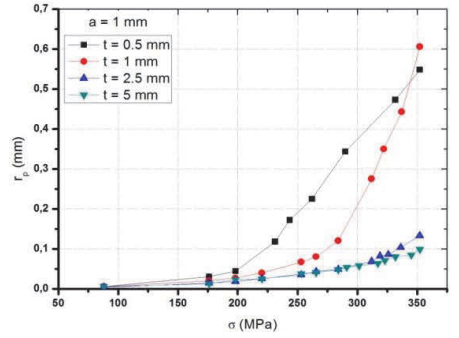

Figure 20: r_p vs σ @ a = 1 mm

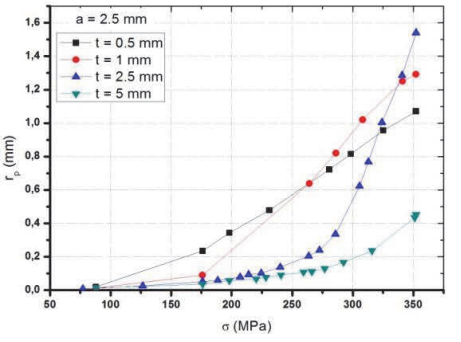

Figure 21: r_p vs σ @ a = 2.5 mm

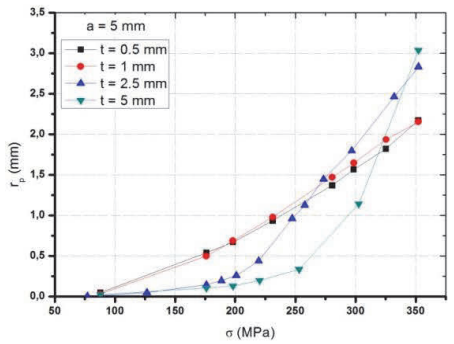

Figure 22: r_p vs σ @ a = 5 mm

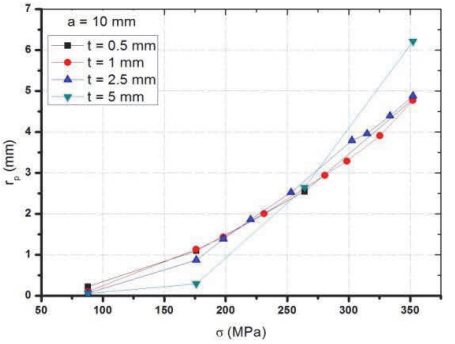

Figure 23: r_p vs σ @ a = 10 mm

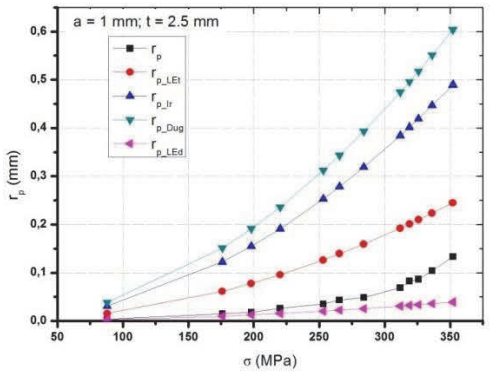

Figure 24: Comparison of r_p vs σ @ a = 1 mm, t = 2.5 mm

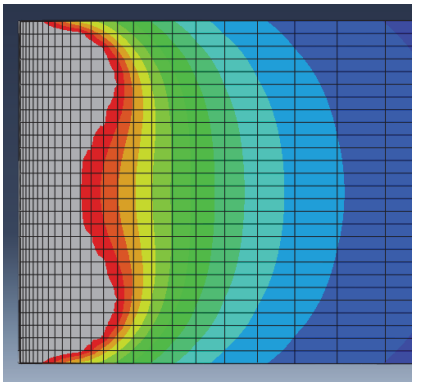

Figure 25: PZS (in grey) along the crack front @ σ = 350 MPa

length, that is in presence SSY condition, J_LE provides results in agreement with the numerical ones (J_Aba); on the contrary, that is in presence of LSY condition, the J_Aba values are higher than J_LE values, as the J_Aba parameter considers the "real" stress-strain state at the crack tip. In Figs. from 16 to 19 it can be seen that the increase of both the applied load value and the crack length lead to an increase of the plastic zone size.

Figs. from 20 to 23 show the influence of thickness on the plastic radius.

It can be seen that for fixed crack length and thickness a load value exists beyond which the plastic radius quickly increases with applied remote load and that load value increases with the thickness and decreases with the crack dimension.

These behaviours can be explained by considering the stress state at the crack tip and then the evolution of plastic zone shape and size along the thickness.

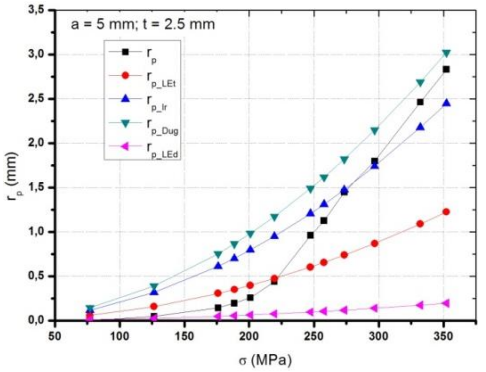

Figure 26: Comparison of r_p vs σ @ a = 5 mm, t = 2.5 mm

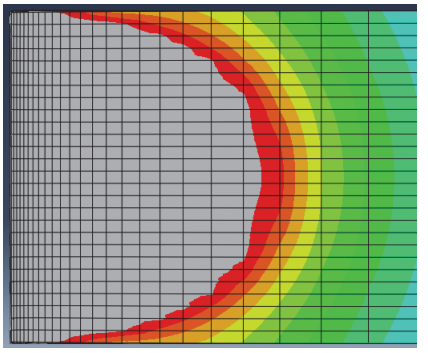

Figure 27: PZS (in grey) along the crack front @ σ = 350 MPa

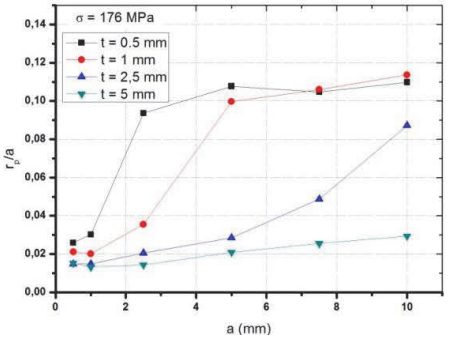

Figure 28: r_p/a vs a @ σ= 176 MPa

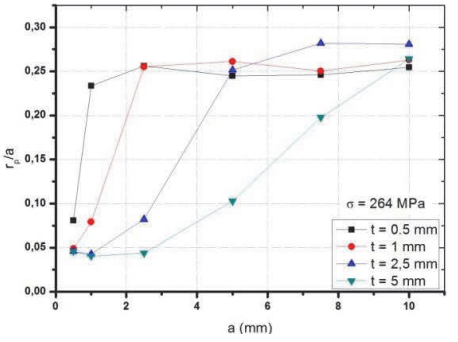

Figure 29: r_p/a vs a @ σ= 264 MPa

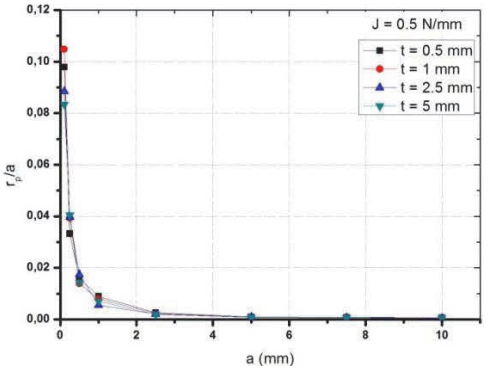

Figure 30: r_p/a vs a @ J= 0.5 N/mm

For what concern the crack tip conditions, in the case of a small applied load or of a short crack the stress state at the crack tip can be considered more similar to a plane strain state; on the contrary, in the case of a high applied load the stress state at the crack tip can be considered more similar to a plane stress state.

For what concern the thickness, being the stress-strain state at the middle plane of the thickness very close to a plane strain one and the plane stress state limited to the outer surfaces, the plastic radius increases slowly with the applied load and its values are confined between the plastic radius values calculated analytically through the LEFM theory by considering plane strain conditions, rp_LEd, and those calculated analytically through the LEFM theory by considering plane stress conditions, rp_LEt (Fig. 24 and Fig. 25).

If the stress state is more similar to a plane stress one, the plastic radius quickly increases with the applied load and reaches the value which can be calculated analytically through the LEFM theory by considering the Dugdale approach, rp_Dug (Figg. 26 and 27).

It can be interesting to consider more deeply the behaviour of the plastic radius with reference to a plate 1 mm thick (Fig. 20): it can be considered, in fact, that the stress state around the crack tip is more similar to the one corresponding to plane stress for a plate 0.5 mm thick and to plane strain for a 2.5 mm thick plate, and it can be observed a transition of the stress state for the 1 mm thick plate from the plane-stress state to the plane-strain one by increasing the applied load value (the same behaviour occurs with an increasing crack length for given plate dimensions).

Figs. 28 and 29 show the influence of the crack length on the ratio between the plastic radius and the length of the same crack (r_p/a) for four different thicknesses, considering the applied load value as fixed. It can be seen that the r_p/a ratio increases with the crack length and the applied load, while it decreases with the thickness.

In Fig. 30 it can be seen that for a fixed value of the J-Integral parameter value (0.5 N/mm) and for different thicknesses the r_p/a ratio decreases as the crack length increases up to a specific crack size; beyond this value PZS becomes constant with the crack size.

This behaviour could justify the use of the PZS as an EPFM parameter for long cracks, as both PZS and the parameter describing the stress state at crack tip, the J-Integral, are constant for that case; for small cracks, in the same conditions, the ratio of PZS to the crack length increases as the crack size decreases, therefore if this ratio is used as a parameter to represent the short crack growth rate, the description should be more coherent with the experimental evidence than the J-Integral or the SIF parameter.

References

Amiri, A.; Belhouari, M.; Bounoua, N.; Achour, T.; Bouiadjra, B. B. (2013): Three-dimensional finite element analysis of thin films cracking along ceramic substrates. *Mech Res Commun*, vol. 47, pp. 1-5.

Anderson, T. (1995): *Fracture Mechanics*, CRC Press.

Armentani, E.; Citarella, R.; Sepe, R. (2011): FML Full Scale Aeronautic Panel Under Multiaxial Fatigue: Experimental Test and DBEM Simulation. *Eng Fract Mech*, vol. 78, pp. 1717-1728.

Bellett, D.; Taylor, D.; Marco, S.; Mazzeo, E.; Guillois, J.; Pircher, T. (2005): The fatigue behaviour of three-dimensional stress concentrations. *Int J Fatigue*, vol. 27, pp. 207–221.

Benedetti, I.; Aliabadi, M. H. (2013): A three-dimensional grain boundary formulation for microstructural modeling of polycrystalline materials. *Computational Materials Science*, vol. 67, pp. 249-60.

Broberg, K. B. (1999): *Cracks and Fracture*, Academic Press.

Camas, D.; Garcia-Manrique, J.; Gonzalez-Herrera, A. (2011): Numerical study of the thickness transition in bi-dimensional specimen cracks. *Int J Fatigue*, vol. 33, no. 7, pp. 921–928.

Caputo, F.; Di Gennaro, F.; Lamanna, G.; Lefons, A.; Riccio, A. (2013): Numerical procedures for damage mechanisms analysis in CFRP composites. *Key Eng Mat*, vol. 569-570, pp. 111-118.

Caputo, F.; Lamanna, G.; Lanzillo, L.; Soprano, A. (2013): Numerical investigation on LEFM limits under LSY conditions. *Key Eng Mat*, vol. 577-578, pp. 381-384.

Caputo, F.; Lamanna, G.; Pannullo, F. M.; De Angelis, G. (2012): A Methodological Approach to the Tolerance Problems during the Assembly Process of Deformable Bodies. *Key Eng Mat*, vol. 488-489, pp. 557-560.

Caputo, F.; Lamanna, G.; Soprano, A. (2013): On the evaluation of the plastic zone size at the crack tip. *Eng Fract Mech*, vol. 103, pp. 162–173.

Caputo, F.; Lamanna, G.; Soprano, A. (2012): Geometrical parameters influencing a hybrid mechanical coupling. *Key Eng Mat*, vol. 525-526, pp. 161-164.

Caputo, F.; Lamanna, G.; Soprano, A. (2012): Effects of Tolerances on the Structural Behavior of a Bolted Hybrid Joint. *Key Eng Mat*, vol. 488-489, pp. 565-569.

Caputo, F.; Lamanna, G.; Soprano, A. (2013): Residual Strength Improvement of an Aluminium Alloy Cracked Panel. *The Open Mechanical Engineering Jour-*

nal, vol. 7, pp. 88-95.

Caputo, F.; Lamanna, G.; Soprano, A. (2011): Numerical modeling and simulation of a bolted hybrid joint. *Structural Durability and Health Monitoring*, vol. 7, no. 4, pp. 283-296.

Caputo, F.; Lamanna, G.; Soprano, A. (2011): An Analytical Formulation for the Plastic Deformation at the Tip of Short Cracks. *Proceedia Engineering*, vol. 10, pp. 2988–2993.

Caputo, F.; Lamanna, G.; Soprano, A. (2006): Numerical Investigation on the Crack Propagation in a Flat Stiffened Panel. *Key Eng Mat*, vol. 324-325, pp. 559-562.

Chang, T.; Hou, G. L. a. J. (2005): Effects of applied stress level on plastic zone size and opening stress ratio of a fatigue crack. *Int J Fatigue*, vol. 27, n. 5, pp. 519–526.

Cisilino, A. P.; Aliabadi, M. H.; Otegui, J. L. (1998): Three-dimensional boundary element formulation for the elastoplastic analysis of cracked bodies. *Int J Numer Meth Eng*, vol. 42, no. 2, pp. 237-256.

Cisilino A. P.; Aliabadi, M. H. (1999): Three-dimensional boundary element analysis of fatigue crack growth in linear and non-linear fracture problems. *Eng Fract Mech*, vol. 63, no. 6, pp. 713-33.

Citarella, R.; Cricrì, G.; Armentani, E. (2013): Multiple crack propagation with Dual Boundary Element Method in stiffened and reinforced full scale aeronautic panels. *Key Eng. Mat.*, vol. 560, pp. 129-155.

Gao, X.; Wang, H.; Kang, X.; Jiang, L. (2010): Analytic solutions to crack tip plastic zone under various loading conditions. *EUR J MECH A-Solid,* vol. 29, no. 4, pp. 738–745.

Hussain, K. (1997): Short fatigue crack behavior and analytical models: a review. *Eng Fract Mech*, vol. 58, pp. 327–54.

Hutchinson, J. W. (1968): Singular behaviour at the end of a tensile crack in a hardening material. *J Mech Phys Solids*, vol. 16, pp. 13-31.

Jin, O.; Mall, S. (2003): Effects of microstructure on short crack growth behavior of Ti–6Al–2Sn–4Zr–2Mo–0.1Si alloy. *Mater Sci Eng*, vol. 359, pp. 356–367.

Kudari, S. K.; Maiti, B.; Ray, K. K. (2009): Experimental investigation on possible dependence of plastic zone size on specimen geometry. *Fract. and Str. Integ,* vol. 7, pp. 57-64.

Lados, D. A.; Apelian, D. (2008): Relationships between microstructure and fatigue crack propagation paths in Al-Si-Mg cast alloys. *Eng Fract Mech*, vol. 75, pp. 821–832.

Lamanna, G.; Caputo, F.; Soprano, A. (2012): Handling of composite-metal interface in a hybrid mechanical coupling. *AIP Conference Proceedings,* vol. 1459, pp. 353-355.

Leitao, V.; Aliabadi, M. H.; Rooke, D. P. (1995): The dual boundary element formulation for elastoplastic fracture mechanics. *Int J Numer Meth Eng*, vol. 38, no. 2, pp. 315-33.

Leitao, V. M. A.; Aliabadi, M. H.; Rooke, D. P. (1995): Elastoplastic simulation of fatigue crack growth. Dual boundary element formulation. *Int J Fatigue*, vol. 17, no. 5, pp. 353-63.

McDowell, D. L. (1997): An engineering model for propagation of small cracks in fatigue. *Eng Fract Mech*, vol. 56, no. 3, pp. 357 - 377.

Narasimhan, R.; Rosakis, A. (1998): Three Dimensional Effects Near a Crack Tip in a Ductile Three Point Bend Specimen. Part 1. A Numerical Investigation. *DTIC Document*.

Newman, J. C.; James, M.; Zerbst, U. (2003): A review of the CTOA/CTOD fracture criterion. *Eng Fract Mech*, vol. 70, pp. 371–385.

Park, H. B.; Kim, K. M.; Lee, B. W.; Rheem, K. S. (1996): Effects of crack tip plasticity on fatigue crack propagation. *J Nucl Mater,* vol. 230, no. 1, pp. 12–18.

Rice, J. R.; Rosengren, G. F. (1968): Plane strain deformation near a crack tip in a power-law hardening material. *J Mech Phys Solids,* vol. 16, pp.1-12.

Sfantos, G. K.; Aliabadi, M. H. (2007): Multi-scale boundary element modelling of material degradation and fracture. *Comput Method Appl M*, vol. 196, no. 7, pp. 1310-29.

Werner, K. (2012): The fatigue crack growth rate and crack opening displacement in 18G2A-steel under tension. *Int J Fatigue*, vol. 39, pp. 25–31.

Zhang, J. Z.; Du, S. Y. (2001): Elastic-plastic finite element analysis and experimental study of short and long fatigue crack growth. *Eng Fract Mech*, vol. 68, no. 14, pp. 1591–1605.